Pharm Res (2014) 31:809–818
DOI 10.1007/s11095-013-1203-4

RESEARCH PAPER

Pharmacokinetics and Pharmacodynamics of CD4-Anchoring Bi-Functional Fusion Inhibitor in Monkeys

Xingrong Liu • Ying C. Ou • Jun Zhang • Ago Ahene • Douglas Clark • Su-Chun Hsieh • Matthew Cooper • Changhua Ji

Received: 16 May 2013 / Accepted: 12 September 2013 / Published online: 25 September 2013

ABSTRACT

Purpose This study was to characterize the pharmacokinetics (PK) and pharmacodynamics (PD) of a chimeric protein, CD4-anchoring bi-functional fusion inhibitor (CD4-BFFI), in monkeys and assess the feasibility for HIV-1 treatment in humans.

Methods The serum concentrations of CD4-BFFI and CD4 receptors were determined and modeled using a target-mediated drug disposition (TMDD) model following intravenous administration of 1 or 10 mg/kg in monkeys. *In vitro* CD4 internalization was examined in human peripheral blood mononuclear cells.

Results Noncompartmental analysis showed a decrease in clearance (1.35 to 0.563 mL/h/kg) and an increase in half-lives (35 to 50 h) with increasing doses. Dose-dependent CD4 occupancy was observed. The TMDD model reasonably captured the PK/PD profiles and suggested greater degradation rate constant for the free CD4 than the bound CD4. *In vitro* assay showed CD4-BFFI did not reduce the internalization of cell surface CD4. The simulated serum concentrations of CD4-BFFI were 20-fold above its *in vitro* IC_{50} for HIV-1 at 3 mg/kg weekly or biweekly following subcutaneous administration in humans.

Conclusions The TMDD modeling and *in vitro* CD4 internalization study indicate that CD4-BFFI does not induce CD4 internalization and CD4-BFFI short half-life is likely due to normal CD4 internalization. The simulated human PK supports CD4-BFFI as a promising anti-HIV-1 agent.

KEY WORDS anti-CD4 monoclonal antibody · bi-functional fusion inhibitor · HIV-1 · modeling · pharmacokinetics/pharmacodynamics

ABBREVIATIONS

ADA	anti-drug antibody
AUC	area under the curve
CD4-BFFI	CD4-anchoring bi-functional fusion inhibitor
ELISA	enzyme-linked immunosorbent assay
FACS	fluorescence-activated cell sorting
HIV-1	human immunodeficiency virus-1
mAb	monoclonal antibody
MFI	mean fluorescence intensity
PBMC	peripheral blood mononuclear cells
PD	pharmacodynamics
PK	pharmacokinetics
TMDD	target-mediated drug disposition
Vdss	steady-state volume of distribution

Electronic supplementary material The online version of this article (doi:10.1007/s11095-013-1203-4) contains supplementary material, which is available to authorized users.

X. Liu (✉) · Y. C. Ou · A. Ahene · D. Clark · S.-C. Hsieh
Department of Drug Metabolism and Pharmacokinetics, Roche Palo Alto
3411 Hillview Avenue, Palo Alto, California 94304 USA
e-mail: liu.xingrong@gene.com

J. Zhang · C. Ji
Department of Viral Diseases, Roche Palo Alto, 3411 Hillview Avenue
Palo Alto, California 94304 USA

M. Cooper
Department of Nonclinical Safety, Roche Palo Alto, 3411 Hillview Avenue
Palo Alto, California 94304 USA

Present Address:
X. Liu
Genentech, Inc., 1 DNA Way South, San Francisco, California 94080
USA

INTRODUCTION

The first human immunodeficiency virus-1 (HIV-1) entry inhibitor on the market, enfuvirtide, is a heptad repeat 2 (HR2) derived peptide that inhibits the fusion process of viral membrane and host cell cytoplasm membrane and prevents the viral entry (1). Enfuvirtide in combination with other agents represents an effective option to counteract resistance mutations for HIV-1 (2, 3). Despite its clinically proven efficacy, the use of enfuvirtide is limited by its twice-daily dosing regimen due to rapid elimination of the peptide from plasma (1, 2, 4). In addition, the low genetic barrier to resistance and injection site reactions in some patients represent challenges in HIV-1 treatment. To overcome these challenges CCR5-anchoring bifunctional fusion inhibitor (CCR5-BFFI) was developed (5). CCR5-BFFI is a chimeric protein and it contains two HIV-1 entry inhibitors: a CCR5 monoclonal antibody (mAb) that blocks HIV-1 attachment to the CCR5 coreceptor and a fusion inhibitor that inhibits the HIV-1 viral-host cell fusion process. CCR5-BFFI showed greater antiviral potency than either the fusion inhibitor peptide or the CCR5 mAb in *in vitro* antiviral assays. However, it failed to block the entry of X4 and R5X4 viruses into HIV-1 target cells expressing CXCR4 coreceptor but not CCR5 coreceptor (5).

To overcome the defect of CCR5-BFFI, we generated a second generation bi-functional fusion inhibitor that is equally potent in inhibiting R5 and X4 HIV-1 viral entry and named it CD4-BFFI (CD4-anchoring bi-functional fusion inhibitor) (6, 7). CD4-BFFI is a chimeric protein consisting of an anti-CD4 mAb, a peptide linker, and a fusion inhibitor peptide T651. The antibody was derived from the sequence of a humanized anti-human CD4 mAb TNX-355 (human IgG_4) (8, 9). In contrast to TNX-355, the anit-CD4 antibody in CD4-BFFI is designed as a human immunoglobulin G1 (IgG_1) isotype, carrying the L234A and L235A double mutations to abolish Fc-mediated antibody-dependent cellular cytotoxicity and complement-dependent cytotoxicity. The HIV-1 fusion inhibitor peptide T651 is recombinantly conjugated to the Fc end of the anti-CD4 antibody via a Glycine-Serine linker. T651 peptide is derived from the heptad repeated 2 (HR2) region of HIV-1 gp41, with two modifications: one internal potential N-glycosylation site was removed by point mutation (N676Q) and a new N-glycosylation site at the N-terminus of the peptide was introduced that leads to improved solubility (6). CD4-BFFI was designed for the treatment of HIV-1 infections by intercepting two different steps of HIV-1 entry process: inhibition of HIV-1 attachment to CD4 receptor by binding to the D2 domain of CD4, and inhibition of HIV-1 fusion by interacting with the HR1 domain of HIV-1 gp41.

CD4-BFFI has demonstrated high and broad antiviral potency *in vitro* and is highly stable in serum (6, 7). It represents a promising therapeutics for HIV-1 infected patients. The objectives of this study were to determine the pharmacokinetics (PK) and pharmacodynamics (PD) of CD4-BFFI in monkeys, characterize the PK/PD relationship using modeling approaches, and assess the feasibility of using CD4-BFFI as a new therapeutics for HIV-1 infections in humans.

MATERIALS AND METHODS

Antibody and Other Chemicals

CD4-BFFI was prepared at Roche Penzberg (Penzberg, Germany) as previously described with a purity of 98.8% (6). All other chemicals used in the experiments were of the highest available grade.

Monkey Study

Male and female cynomolgus monkeys weighing 3–7 kg were obtained from Charles River (Biomedical Resources Foundation). CD4-BFFI (3.8 mg/mL) was prepared in an aqueous vehicle containing 20 mM histidine and 140 mM sodium chloride at pH 6. Three male cynomolgus monkeys were dosed intravenously (IV) at 1 or 10 mg/kg CD4-BFFI. Blood samples were taken before dosing and at 15 min, 30 min, 1, 3, 6, 24, 48, 72, 96, 168, 336, and 504 h after dosing from the femoral vein. For multiple dose study, 2 male and 2 female monkeys were dosed every 3 days on day 1, 4, 7, 10, and 13. On days 1 and 13, blood samples were collected from all animals pre-dose and at 4, 24, 48, and 72 h after dosing. Blood samples were maintained at room temperature and allowed to clot. Serum was prepared in a refrigerated centrifuge (10°C) within 2 h of blood collection. All procedures involving animals were approved by the Institutional Animal Care and Use Committees at Roche Palo Alto.

Determination of Serum CD4-BFFI

Concentrations of CD4-BFFI in serum were determined by a specific ELISA method in 96-well plates. Briefly, the serum samples and the calibration standards were incubated in 96-well plates which contain immobilized heptad repeat 1 (HR1) peptide at 25°C for 1 h. After the plates were washed 3 times, a digoxiginated anti-human IgG-pan mAb against the human antibody Fcγ region was added into the wells and the plates were incubated at 25°C for 1 h. After the plates were washed 3 times, a horseradish peroxidase (HRP) linked mAb against digoxigenin was added into the wells and the plates were incubated at 25°C for 1 h, and then washed for 3 times. Finally, HRP substrate 2,2'-azino-di-(3-ethylbenzthiazoline-6-sulfonic acid) (ABTS) in hydrogen peroxide was added into the wells and the plates were incubated at 25°C for 15 min. The absorbance was detected at 409 nm with a plate reader. The accuracy of the method as calculated from the recoveries of the quality control samples (% Theoretical) of CD4-BFFI which

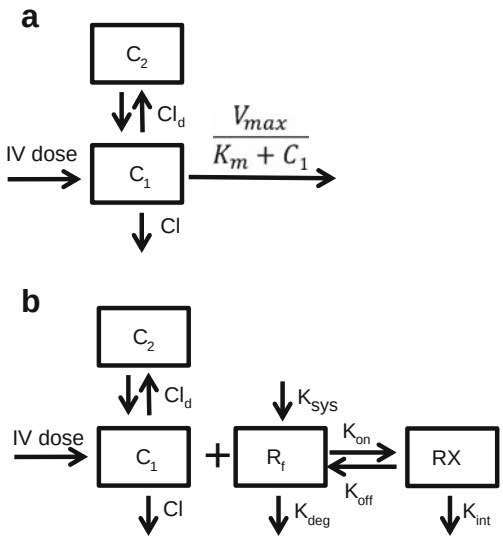

Fig. 1 Schematic representation of two-compartmenal PK model (**a**) and target mediated drug disposition (TMDD) model (**b**). CL, linear clearance from the central compartment; Cl_d, inter-compartment distribution clearance; Vmax, maximal rate of elimination; Km, Michaelis-Menton constant. Free CD4 receptor (Rf) were modeled to form a drug-receptor complex (XR) via reversible (K_{on} and K_{off}) binding, and the complex was eliminated by cellular internalization (K_{int}). CD4 receptor synthesis rate was K_{syn} and degradation rate as K_{deg}.

ranged from 96.5% to 100.1%. Calibration standards for CD4-BFFI in monkey serum ranged from 7 to 100 ng/mL.

Determination of Serum CD4

Whole blood (200 μL) from three monkeys before and after dosing with CD4-BFFI was incubated with 5 μg/mL mouse anti-human CD4 mAb OKT4-Pacific Blue (BioLegend, San Diego, CA) or Alexa-488 labeled CD4-BFFI on ice for 45 min. The Alexa-488 labeled CD4-BFFI was covalently labeled with fluorochrome Alexa 488 following procedure from Alexa Fluor 488 MAb Labeling Kit from Invitrogen (Invitrogen). The red blood cells were removed by incubation in 1 mL of 1X lysis buffer (BD PharmLyse lysing buffer (10X), BD Biosciences, San Diego, CA) for 15–20 min followed by centrifugation for 5 min at 300 g. The pellet was washed with 250 μL FACS (fluorescence activated cell sorting) staining buffer (PBS containing 3% heat-inactivated fetal calf serum, 0.09% (w/v) sodium azide) and the CD4 staining on monkey peripheral blood mononuclear cells (PBMC) was analyzed by Fluorescence-activated cell sorting (FACS). For the calculation of CD4 occupancy, the mean fluorescence intensity (MFI) from the pre-dose samples were set as 0% CD4 occupancy and MFI from the pre-dose samples treated with saturating amount of CD4-BFFI before adding Alexa-488 labeled CD4-BFFI was set as 100% occupancy. MFI from OKT4-Pacific Blue staining was used to assess the total CD4 level on the PBMC. OKT4 binds to D3/4 domains of CD4 and CD4-BFFI binds to D2 domain of CD4. It has been reported that OKT4 and TNX-355 do not compete for binding to CD4 (10), therefore OKT4 was used to determine the total CD4 (both CD4-BFFI bound and free CD4) in CD4-BFFI dosed monkey blood samples.

In Vitro CD4 Internalization Assay

Commercial fluorochrome-labeled anti-human CD4 mAbs OKT4, MT-310, and B486A1 were purchased from BD Biosciences (La Jolla, CA). Human PBMCs from healthy donors were purchased from AllCells (cat # PB001, Emeryville, CA) and cultured in complete medium (RPMI 1640, 10% FBS, 1% P/S, 1% L-Glutamine, 1% non-essential amino acid, 1% sodium pyruvate, 1% HEPES, 5 IU/mL IL-2). PBMC at 2×10^{-6} cells/mL were treated with cycloheximide at 10 μg/mL final concentration and distributed onto a multiwell plate on ice. Labeled various CD4 antibodies were added to the cells at 1 μg/reaction/200 μL on ice. Two hundred μL reaction solution was kept at 4°C as time 0. The rest binding reaction solutions were incubated at 37°C for various time points. At the end of each incubation time point, the corresponding reaction wells were kept at 4°C to stop the internalization. After all time points were collected, cells were spun down and washed 3 times and re-suspended in ice cold 300 μL FACS buffer. Samples were analyzed by using FACS Calibur (BD, San Jose, CA) and data were processed using FlowJo (Tree Star, Ashland, OR).

Data Analysis

PK parameters were determined using noncompartmental method with WinNonlin Professional software (version 5.2.1; Pharsight, Mountain View, CA) and were based on individual subject serum concentration-time data. PK parameters including terminal half-life ($t_{1/2}$), area under the curve from time zero to the last time ($AUC_{(0\text{-last})}$), AUC from time zero to infinity ($AUC_{(0\text{-}\infty)}$), clearance (Cl), and steady-state volume of distribution (Vdss) were calculated.

Two-Compartment Michaelis-Menten PK Model

A two-compartment PK model with Michaelis-Menten kinetics (Fig. 1a) was used to characterize the nonlinear clearance. Like other mAbs targeting membrane-associated antigens, CD4-BFFI is expected to have two distinct elimination pathways *in vivo* (11–13). One pathway is nonspecific antibody elimination through intracellular degradation, which is protected by FcRn-mediated endosomal recycling. The other pathway is receptor-mediated internalization of antibody-receptor complex, which is saturable because of the limited availability of CD4 receptors on the cell surface.

CD4-BFFI in the central compartment was assumed to be eliminated by both linear clearance and nonlinear clearance in Eq. 1.

$$Clearance = Cl + \frac{V_{\max}}{K_m + C_1} \quad (1)$$

Where Cl represents linear clearance, V_{max} and K_m represent maximal rate of elimination and Michaelis-Menten constant for the nonlinear clearance, and C_1 represents CD4-BFFI concentration in the central compartment.

The drug concentration in the central compartment following IV bolus dose was described by Eq. 2:

$$V_1\frac{dC_1}{dt} = Cl_d \bullet C_2 - \left(Cl_d + Cl + \frac{V_{\max}}{K_m + C_1}\right)\bullet C_1 \quad (2)$$

where V_1 is the volume of distribution in the central compartment, Cl_d is the distribution clearance between central and peripheral compartment.

The drug concentration in the peripheral compartment was described by Eq. 3:

$$V_2\frac{dC_2}{dt} = Cl_d \bullet (C_1 - C_2) \quad (3)$$

where C_2 is the concentration in the peripheral compartment and V_2 is the volume of distribution in the peripheral compartment. Due to a small sample size in our studies (6 monkeys) and 6 parameters to be estimated from Michaelis-Menten PK model, we employed a population NONMEM approach. The Individual fitting using Berkeley Madonna software had non-identifiable issues (not enough data for proper model estimation). The advantage of population/NONMEM approach is that population mean estimate can be used to help identify individual parameter estimation. The population model implemented in NONMEM (Version 6.2, ICON, Dublin, Ireland) was used to simultaneously fit the data from the 1 mg/kg and 10 mg/kg dose groups. Selection of final model was based on Objective Function and Akaike Information Criterion (AIC) for nested models. In addition, several diagnostic plots including model prediction (IPRED) *vs.* observed data (DV) and non-biased distribution of IWRES were also evaluated.

Target-Mediated Drug Disposition (TMDD) Model

TMDD modeling approach and its framework were described in the literature (11–13). In brief, concentrations of CD4-BFFI in the central compartment (C_1) and free CD4 receptor (R_f) formed a drug-receptor complex (XR) via reversible binding with on-rate constant K_{on} and off-rate constant K_{off}, and the complex was eliminated by cellular internalization (K_{int}). The configuration of the TDMM model is shown in Fig. 1b. The drug concentration in the central compartment following IV bolus dose was described by Eq. 4:

$$V_1\frac{dC_1}{dt} = Cl_d \bullet C_2 - (Cl_d + Cl) \bullet C_1 - \left(K_{on}C_1R_f - K_{off}XR\right)\bullet V_1 \quad (4)$$

The drug concentration in the peripheral compartment was described by Eq. 3.

The R_f concentration was described by Eq. 5:

$$\frac{dR_f}{dt} = K_{syn} - K_{\deg} \bullet R_f - K_{on} \bullet C_1 \bullet R_f + K_{off} \bullet XR \quad (5)$$

Where K_{syn} and K_{deg} represent the rate constants of CD4 synthesis and degradation, respectively.

The concentration of XR was described by Eq. 6:

$$\frac{dXR}{dt} = K_{on} \bullet C_1 \bullet R_f - K_{off} \bullet XR - K_{\text{int}} \bullet XR \quad (6)$$

To avoid non-identifiable issues (a total of 8 parameters to estimate from 6 monkeys), we used a stepwise approach and assumed that the difference between TMDD and Michaelis-Menten model is the non-linear clearance pathway mediated by the receptor binding. The PK parameters Cl, Cl_d, V_1 and V_2 were fixed to the same estimated values from the two-compartment Michaelis-Menten model. TMDD model was simultaneously fitted to individual serum concentration-time profiles of CD4-BFFI, free, and total CD4 to estimate R_0 (initial free CD4 concentration), K_{deg}, K_{int} and K_{on}. K_{syn} was set at $K_{syn} = R_0 * K_{deg}$. Monkey K_d of 0.020 μg/mL (Supplementary Material Figure 1) was used to estimate K_{off} based on $K_{off} = K_d * K_{on}$. The model was implemented in Berkeley Madonna (Version 8.3, University of California at Berkeley, Berkeley, CA) and parameter estimates were based on minimization of least mean square errors. While we were also able to implement the TMDD model in NONMEM with same fixed parameters, the population/NONMEM approach did not yield satisfactory description of data due to number of parameters needed to be estimated from a small number of animals.

Human PK Simulation

To simulate human PK for CD4-BFFI after subcutaneous (SC) administration, allometry scaling was used based on model parameters obtained from the two-compartment model and TMDD model. Allometry exponent was set as 1 for the volume of distribution (V_1 and V_2) and allometry exponent was set as 0.85 for the linear clearance (Cl) and inter compart distribution clearance (Cl_d) for both the two-compartment and TMDD models. For the two-compartment model, human V_{max} was estimated from monkey V_{max} and human K_m was estimated form the product of monkey K_m and $K_{d(human)}/K_{d(monkey)}$ ratio, where $K_{d(human)}$ and $K_{d(monkey)}$ are the observed disassociation constants for human and monkey CD4

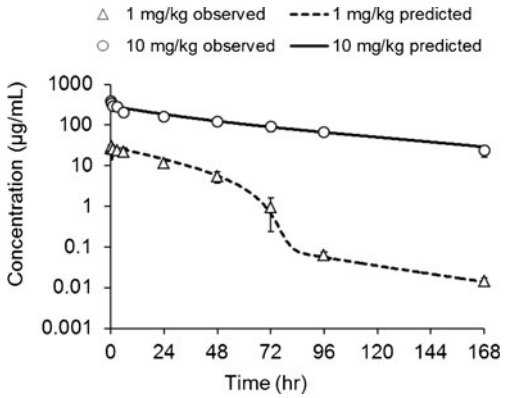

Fig. 2 Serum concentration-time profiles of CD4-BFFI following a single IV dosing of 1 mg/kg or 10 mg/kg in cynomolgus monkeys. The *symbols* represent the observed data (mean ± SD) and the *lines* represent the best fit of the two-compartment model shown in Fig. 1a to the observed data.

receptor, respectively. For the TMDD model, all the human CD4 targeted related parameters were assumed same as the monkey parameters except the K_d, for which human value was used.

RESULTS

CD4-BFFI PK and Modeling Following a Single IV Administration in Monkeys

CD4-BFFI was well tolerated following a single IV dose of 1 mg/kg or 10 mg/kg in monkeys and exhibited nonlinear PK (Fig. 2). The clearance at 1 mg/kg was 2.4-fold greater than that at 10 mg/kg. The estimated mean $t_{1/2}$ was 35 h at 1 mg/kg and 50 h at 10 mg/kg (Table I). A two-compartment Michaelis-Menten PK model illustrated in Fig. 1a with both linear and nonlinear clearance from the central compartment was able to fit the plasma concentration-time data (Fig. 2). The goodness-of-fit was presented in Supplementary Material Figure 2. The mean PK parameters are listed in Table II.

Table II CD4-BFFI PK Parameters of the Two-Compartment PK Model Following a Single IV Administration in Cynomolgus Monkeys

Parameter	Unit	Estimate (RSE%)
Cl	mL/h/kg	0.398 (9%)
Cl_d	mL/h/kg	0.287 (3%)
V_1	mL/kg	34.0 (2%)
V_2	mL/kg	15.9 (3%)
V_{max}	μg/h/kg	8.36 (3%)
K_m	μg/mL	0.352 (6%)

RSE Relative standard error

CD4-BFFI PK Following Multiple IV Administrations in Monkeys

Similar to the single dose study, after multiple IV doses at 1 mg/kg or 10 mg/kg every 3 days for 13 days, CD4-BFFI exhibited nonlinear PK with 4.0-fold higher clearance at 1 mg/kg than that at 10 mg/kg on day 1 (Table I). The terminal $t_{1/2}$ at 1 mg/kg in the single dose study was longer than the terminal $t_{1/2}$ at the same dose level in the multiple dose study on day 1 (35 h *vs.* 8 h). In contrast, the terminal $t_{1/2}$ at 10 mg/kg in single dose study was similar to that in the multiple dose study on day 1 (58.0 h *vs.* 58.1 h). The apparent difference of the $t_{1/2}$ between the single dose and multiple dose studies at 1 mg/kg but not at 10 mg/kg are due to the difference of the time points that are available for calculation of the $t_{1/2}$. In the single dose study, the sera were collected from 0 h to 504 h and concentration data are available from 0 h to 168 h with concentration at 336 h and 504 h below the lower limit of the quantitation. In the multiple dose study, the sera were only collected from 0 h to 72 h.

The exposure on day 13 was lower than that on day 1 for the 1 mg/kg group (Table I). On day 13, only concentrations at 4 h were detectable in 3 of the 4 monkeys at 1 mg/kg. To test if the decrease of exposure after multiple doses was due to formation of anti-drug antibody (ADA) in the monkey serum,

Table I Non-Compartment Pharmacokinetic Parameters (Mean ± SD) of CD4-BFFI Following IV Administration in Cynomolgus Monkeys

Dose regimen	Time (day)	Dose (mg/kg)	$t_{1/2}$ (hr)	AUC $_{(0\text{-}t)}$ (μg*hr/mL)	AUC $_{(0\text{-}\infty)}$ (μg*hr/mL)	Cl (mL/h/kg)	Vdss (mL/kg)
Single[a]	1	1	35.0 ± 5.0	751 ± 120	752 ± 120	1.35 ± 0.21	28.4 ± 2.6
Single[a]	1	10	50.0 ± 6.9	16200 ± 1800	18000 ± 2600	0.563 ± 0.080	39.4 ± 1.1
Multiple[b]	1	1	8.31 ± 0.38	339 ± 43	340 ± 43	2.97 ± 0.37	37.9 ± 4.7
Multiple[b]	1	10	58.1 ± 1.9	8220 ± 820	13700 ± 1600	0.746 ± 0.080	58.5 ± 5.6
Multiple[b]	13	1	4.34[c]	164[c]	164[c]	6.11[c]	29.4[c]
Multiple[b]	13	10	39.2 ± 13.8	13192 ± 2989	18041 ± 5812	0.609 ± 0.232	28.6 ± 4.6

$t_{1/2}$ terminal half-life, $AUC_{(0\text{-}t)}$ area under curve from time zero to the last measurable time point, $AUC_{(0\text{-}\infty)}$ area under curve from time zero to infinity, *Cl* clearance, *Vdss* steady-state volume of distribution

[a] $N = 3$

[b] $N = 4$, dosed every 3 days

[c] Concentrations were above the lower limit of quantitation in only one of the four animals

Table III Recovery of the CD4-BFFI in Monkey Serum Following a Single IV Administration in Cynomolgus Monkeys

Time	1 mg/kg			10 mg/kg		
	Monkey Q	Monkey R	Monkey S	Monkey T	Monkey U	Monkey V
Predose	100%	100%	100%	100%	100%	100%
Day 14	0.00%	69.7%	3.37%	0.00%	0.00%	0.00%
Day 21	0.00%	18.4%	3.14%	0.00%	0.00%	0.00%

The recovery was conducted by adding 0.1 μg/mL of CD4-BFFI into the monkey serum collected pre-dose, and days 14 and 21 after dosing

CD4-BFFI recovery was examined in serum samples previously collected at predose, 336 h (day 14), and 504 h (day 21) from the monkeys in the single dose study. For the monkey sera collected prior to CD4-BFFI administration, the recovery was 100% for all the 6 monkeys. The recovery was reduced after the administration of CD4-BFFI (Table III). At 1 mg/kg, the recovery reduced to 0–69.7% on day 14 and 0–18.4% on day 21. At 10 mg/kg, the recovery reduced to 0% on days 14 and 21. Due to limited volume of sera from the multiple dose study, the recovery assay was not performed for those serum samples.

CD4 Concentrations Following a Single IV Administration of CD4-BFFI in Monkeys and TMDD Modeling

One day after the administration of CD4-BFFI, free receptor was reduced to less than 10% of the baseline indicating greater than 90% receptor occupancy by CD4-BFFI (Fig. 3). The free CD4 receptors gradually returned to the predose level in about 168 h (7 days) at 1 mg/kg (Fig. 3a) but were still less than the predose level at 10 mg/kg (Fig. 3b). In contrast, the total CD4 receptors quickly increased and reached to the maximal levels at approximately 6 h and then it reduced and maintained at 30–50% above the baseline.

The TMDD model reasonably describes the serum concentrations of CD4-BFFI, the free CD4, and the trend of the total CD4 (Fig. 3). The goodness-of-fit was presented in Supplementary Material Figure 3. The model parameters are shown in Table IV. The TMDD modeling analysis showed that the internalization rate constant of the bound CD4 which is the complex of CD4-BFFI and CD4 receptors, K_{int} (0.0237 h^{-1}), was slightly less than the degradation rate constant of the free CD4, K_{deg} (0.0397 h^{-1}), suggesting CD4-BFFI did not induce the CD4 internalization. To examine the robustness of this observation, a sensitivity analysis was conducted using the model to simulate the effects of different K_{int} on the total CD4 (Fig. 4a). As shown in Fig. 4a, K_{int} would need to be smaller than K_{deg} in order to describe the elevation of the total CD4 above the baseline following CD4-BFFI administration. In the TMDD model, the CD4 receptor synthesis rate was assumed to be constant. Additional modeling exercise indicated that the elevation of the total CD4 above the baseline can also be explained by an increased synthesis rate of CD4 (k_{syn}) following CD4-BFFI administration (Fig. 4b).

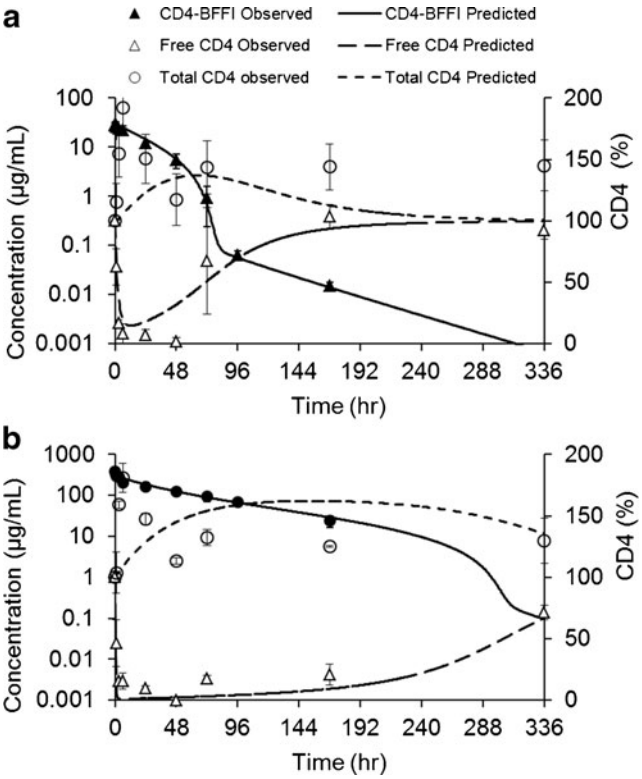

Fig. 3 Serum concentration-time profiles of CD4-BFFI, free CD4, and total CD4 following a single IV dosing of 1 mg/kg (**a**) or 10 mg/kg (**b**) in cynomolgus monkeys. The *symbols* represent the observed data (mean ± SD) and the *lines* represent the best fit of the TMDD model shown in Fig. 1b to the observed data.

In Vitro Assessment of CD4 Receptor Internalization

In order to accurately monitor surface CD4 levels over a long period, cycloheximide was used to block *de novo* CD4 protein

Table IV CD4-BFFI TMDD Model Parameters Following a Single IV Administration in Cynomolgus Monkeys

Parameter	Unit	Mean (CV%)
Cl (fixed)	mL/h/kg	0.398
Cl_d(fixed)	mL/h/kg	0.287
V_1(fixed)	mL/kg	34.0
V_2(fixed)	mL/kg	15.9
R_o	nM	0.0565 (38.2%)
K_{deg}	hr^{-1}	0.0397 (16.2%)
K_{on}	nM/h	2.45 (37.4%)
K_{int}	hr^{-1}	0.0237 (17.6%)

K_d of 0.020 μg/mL was used to estimate K_{off} based on $K_{off} = K_{on}*K_d$

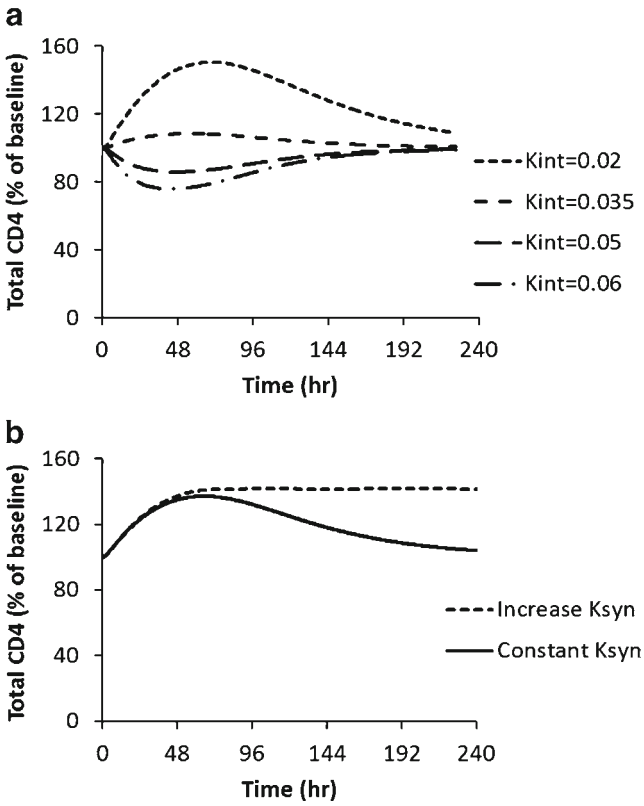

Fig. 4 Simulated concentration-time profiles of total CD4: (**a**) effects of different internalization rate constants (K_{int}) of the bound CD4 on the total CD4 and (**b**) effects of different CD4 synthesis rate constants (K_{sys}) on the total CD4 following a single IV dosing at 10 mg/kg.

synthesis in PBMCs. If an antibody induces CD4 internalization and degradation, the fluorescence, which represent the total surface CD4 level, will decrease over time. As shown in Fig. 5, the fluorescence of two cells treated with MT310 and B486A reduced over time, indicating induction of CD4 internalization and degradation in the PBMCs. However, CD4-BFFI and OKT4 did not cause any observable reduction of the fluorescence, indicating no induction of CD4 internalization in the PBMCs for these two mAbs.

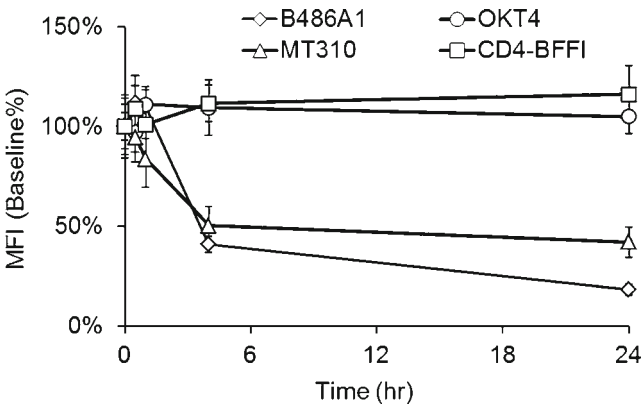

Fig. 5 Effects of mAb B486A1, OKT4, and MT310 and CD4-BFFI on the MFI measured by FACS. MFI indicates the total CD4 receptors on the surface of the human PBMC.

CD4-BFFI Human PK Simulation

To assess the feasibility of development of CD4-BFFI as a human therapeutic protein to treat HIV-1, human PK of CD4-BFFI after SC administration was simulated based on the model parameters obtained from the two-compartment Michaelis-Menten model (Table II). For the volume of distribution, the allometry exponent was set as 1, predicting human volume of distribution for the central compartment and peripheral compartment of 34 mL/kg and 15.9 mL/kg, respectively. For the linear clearance, the exponent was set as 0.85, resulting in projected human linear clearance of 0.249 mL/h/kg. For the nonlinear clearance in the two-compartment model, the human K_m (0.546 μg/mL) was scaled based on monkey K_m (0.352 μg/mL) corrected for the difference of monkey and human K_d where K_d for human CD4 is 0.031 μg/mL and K_d for monkey CD4 is 0.020 μg/mL (Supplementary Material Figure 1). For the nonlinear clearance in the TMDD model, all the human CD4 targeted related parameters were assumed

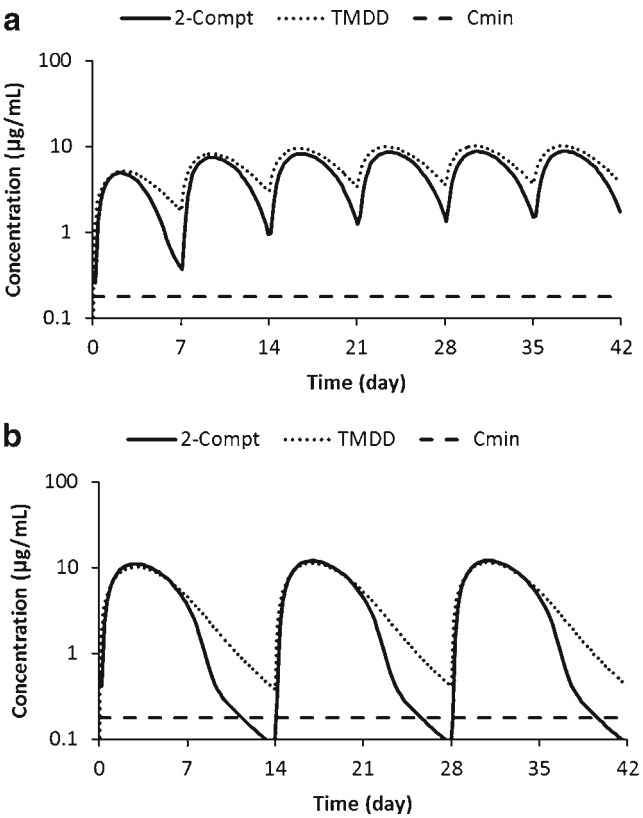

Fig. 6 Simulated human serum concentration-time profiles of CD4-BFFI following 3 mg/kg weekly (**a**) or biweekly (**b**) SC administration using the 2-compartment model (*solid line*) or the TMDD model (*dotted line*). The C_{min} (0.182 μg/mL) represents 20-fold of the observed *in vitro* IC_{50} (0.0091 μg/mL) for blocking HIV-1 infections in PBMCs. Bioavailability is assumed as 50%–75% and K_a is assumed as 0.01−0.03 h^{-1}.

same as the monkey parameters except the K_d, for which human value was used. The absorption rate constant and bioavailability following a SC dosing were assumed as 0.01 to 0.03 h^{-1} and 50 to 75%, respectively. These values were based on other known human IgG mAbs in humans (14). In order to achieve sufficient clinical efficacy, we assume the minimal serum concentration of CD4-BFFI needs to be 20-fold higher than the observed *in vitro* IC_{50} (0.0091 μg/mL) for blocking HIV-1 infections in PBMCs (7). Under these assumptions, human plasma concentration-time profiles were simulated using both the two-compartment model and TMDD model (Fig. 6) at 3 mg/kg weekly or biweekly administration. The predicted human concentration-time profiles using the two-compartment approach and TMDD approach are similar. The projected human terminal $t_{1/2}$ is 30–90 h.

DISCUSSION

CD4-BFFI showed nonlinear PK at dose range of 1 to 10 mg/kg in monkeys. Similar to other anti-CD4 antibody reported in the literature, it has $t_{1/2}$ of approximate 2 days in monkeys. After multiple doses, its clearance increased likely due to formation of ADA in monkeys. Dose-dependent CD4 occupancy was observed with CD4-BFFI. The occupancy for the CD4 receptors was greater than 90% for 2 and 7 days after single IV administration in monkeys at 1 and 10 mg/kg, respectively. The results of the TMDD modeling and the *in vitro* CD4 internalization study showed that binding of CD4-BFFI to CD4 does not stimulate CD4 internalization and degradation. The simulated human PK supports CD4-BFFI may reach efficacious serum concentrations at 3 mg/kg.

CD4-BFFI Showed Nonlinear PK in Monkeys

CD4-BFFI exhibited nonlinear PK at doses from 1 to 10 mg/kg in monkeys following IV administration. The nonlinear is likely due to saturable binding to CD4 receptors and degradation. A two-compartment PK model with both linear and nonlinear clearance from the central compartment was able to fit the observed 1 mg/kg and 10 mg/kg data simultaneously. After multiple dose at 1 mg/kg, CD4-BFFI exhibited lower exposure on day 13 as compared to day 1. We hypothesized the decrease of the exposure after multiple doses was due to formation of ADA in the monkey serum. Since an assay for measuring monkey ADA against CD4-BFFI was not available, we used the CD4-BFFI recovery as a surrogate approach to indicate the formation of ADA in the monkey serum. If ADA exists in the sera, the recovery should be less than 100% because our specific CD4-BFFI assay requires intact and unbound CD4 antibody and functional fusion peptide. We observed the recovery was 100% in all the pre-dosed monkey sera but reduced in the post-dosed sera, indicating sequestration of the spiked CD-BFFI, likely due to the presence of the formation of ADAs in the post-dosed monkey sera.

Mechanism of the Short $t_{1/2}$ of CD4-BFFI in Monkeys

The $t_{1/2}$ of CD4-BFFI in monkeys is approximate 2 days. Typically the $t_{1/2}$ for an IgG is from a few days to 20 days in monkeys (15, 16). A similar anti-CD4 mAb, TNX 355, without the linker and fusion peptide, showed similar $t_{1/2}$ with 15 h at 1 mg/kg and 99 h at 10 mg/kg in monkeys (8, 9). The similar $t_{1/2}$ for CD4-BFFI and TNX 355 are similar in their corresponding doses, suggesting the relatively short $t_{1/2}$ of CD4-BFFI is likely related to the binding to CD4.

Short $t_{1/2}$ has been reported for another anti-CD4 mAb, TRX1, a CD4 non-depleting mAb (12, 17). It was hypothesized that the short $t_{1/2}$ for TRX1 was due to its induction of CD4 internalization as the free and total CD4 were reduced following TRX1 administration in humans (9, 12). Following administration of CD4-BFFI, only the free CD4 was reduced and the total CD4 was maintained and stayed above the predose level, suggesting that the short $t_{1/2}$ of CD4-BFFI was not due to the induction of the internalization and degradation of CD4-BFFI and CD4 complex. Instead, the short $t_{1/2}$ is likely due to the normal internalization and catabolism of CD4 receptor, enhancement of CD4 synthesis, or trafficking.

Development of a TMDD model allowed us to further examine the PK/PD of CD4-BFFI. It has been shown that CD4 has slow endocytosis and turnover in lymphocytes (18). As the estimated K_{int} from the TMDD modeling was slightly less than the estimated K_{deg}, indicating CD4-BFFI did not stimulate CD4 internalization. Instead the mAb followed the normal turnover rate of the CD4 receptor. *In vitro* receptor internalization results are consistent with the *in vivo* modeling results. Binding of CD4-BFFI to CD4 did not cause internalization of CD4 in human PBMCs *in vitro* for 24 h in our *in vitro* internalization assay. As a comparison, Ng *et al.* (12) observed that TRX1 induced CD4 internalization in 30 min after incubation with T cells *in vitro*. Another possibility is that an increase of cell surface CD4, which can be achieved by increasing the de novo synthesis or trafficking, may contribute to the short $t_{1/2}$ for CD4-BFFI. This modeling showed that the TMDD modeling is a useful tool to quantitatively examine the observed results under different assumptions.

Simulated Human PK Supports CD4-BFFI as a Promising Anti-HIV-1 Agent

To assess the feasibility of development of CD4-BFFI as a new therapeutic for treating HIV-1 patients, we simulated its human PK following SC administration based on model parameters from the two-compartment Michaelis-Menton PK modeling coupling using allometric scaling. The SC route is considered as the most likely route to dose protein drug in clinical settings. It

has been reported in the literature that allometry is a useful approach to simulate human PK for therapeutic mAbs (15, 16, 19). We used allometric scaling approach based on monkey PK data with exponent of 0.85 for clearance and exponent of 1 for volume of distribution. This approach was supported by several studies reporting a better prediction of human PK based on monkey PK data and an allometric scaling exponent of 0.85 for clearance than other scaling approaches (14, 20–22). Although two-compartment allometry approach has been used successfully in prediction of human PK for mAb with nonlinear PK when the plasma concentrations were greater than the K_m, it tends to overestimate the human plasma concentration when the human plasma concentrations were less than the K_m (19). Recently Luu *et al.* (23) described a TMDD allometry method that successfully predicted the human concentration-time profile for a mAb. In this method, the PK parameters such as distribution rate constants in the TMDD model were predicted using allometry, the receptor related parameters in the TMDD model were from the observed *in vitro* values, and the receptor concentration was from monkey. In the present work, the predicted human PK was similar using both methods, supporting CD4-BFFI can be used as a viable agent HIV-1 treatment. A number of therapeutic mAbs bind both human and primate antigens, but not the homologous murine antigens. Therefore, allometric scaling based on primate PK alone could provide the most relevant information for the prediction of human PK of humanized antibodies.

The projected the human terminal half-life to be 30–90 h at 3 mg/kg of doses. These values are comparable or longer than the human $t_{1/2}$ for a related CD4 antibody, TNX 355, whose human $t_{1/2}$ was 8 h at 1 mg/kg and 29 h at 10 mg/kg (9). As compared to the current 90 mg twice daily dose regimen for fusion inhibitor enfuvirtide (1–4), CD4-BFFI will clearly provide significant advantages for its enhanced efficacy, better compliance, and higher hurdle of drug resistance.

Receptor expression levels are known to be different between healthy volunteers and HIV-1-infected patients. It has been reported that HIV-1 infection down-regulates CD4, most likely through HIV-1 virulence factor nef. HIV-1 nef-induced CD4 down regulation probably via two mechanisms: accelerated endocytosis and degradation, and direct routing from the Golgi apparatus to the endocytic pathway (24–26). HIV-1 nef also induce MHC-I endocytosis and degradation, possibly as a mechanism of immune evasion through reduced viral antigen presentation and recognition by effector immune cells (27). The fact that CD4-BFFI do not interfere with the T cell receptor coreceptor function of CD4 (8, 28) and increase total CD4 density on lymphocytes may help combat the nef-mediated negative immunomodulatory effects. HIV-1-infected patients will lose both CD4 expression and CD4 T cells. During early stage infection only moderate reduction of CD4 counts is observed, AIDS (acquired immunodeficiency syndrome) patients are accompanied with a rapid and steady decline of CD4 T cell counts to ≤200 cells/μL, ≥80% lower than the normal baseline level (29). The reduced CD4 target in HIV-1 chronically infected especially late stage AIDS patients will likely result in reduced target-mediated clearance of the CD4-BFFI; therefore, these patients may need lower doses or less frequent dosing than the projected human doses.

In summary, CD4-BFFI exhibited nonlinear PK in monkeys in the dose range of 1 to 10 mg/kg following IV administration with a $t_{1/2}$ of 35 to 50 h. Its exposure reduced after multiple doses, likely due to the formation of ADAs in monkeys. Unlike other anti-CD4 antibody TRX1, CD4-BFFI did not induce internalization and degradation after binding to CD4. Based on the monkey PK results and *in vitro* antiviral potency, CD4-BFFI may be efficacious in HIV-1 infected patients at 3 mg/kg using a weekly or bi-weekly dosing schedule. Therefore, the present study supports continuous development of CD4-BFFI as a new therapeutics for the treatment of HIV-1 infections.

ACKNOWLEDGMENTS AND DISCLOSURES

The authors thank our Roche colleagues Friederike Hesse and Erhard Kopetzki for providing the CD4-BFFI, Surya Sankuratri, Stefan Ries, Rubas Werner, Grace Cruz, and Danlin Wu for their contribution and support, and Christophe Meilli for helpful discussion regarding PK/PD model development.

REFERENCES

1. Kilby JM, Hopkins S, Venetta TM, DiMassimo B, Cloud GA, Lee JY, *et al*. Potent suppression of HIV-1 replication in humans by T-20, a peptide inhibitor of gp41-mediated virus entry. Nat Med. 1998;4(11):1302–7.
2. Lazzarin A. Enfuvirtide: the first HIV fusion inhibitor. Expert Opin Pharmacother. 2005;6(3):453–64.
3. Borkow G, Lapidot A. Multi-targeting the entrance door to block HIV-1. Curr Drug Targets. 2005;5(1):3–15.
4. Marr P, Walmsley S. Reassessment of enfuvirtide's role in the management of HIV-1 infection. Expert Opin Pharmacother. 2008;9(13):2349–62.
5. Kopetzki E, Jekle A, Ji C, Rao E, Zhang J, Fischer S, *et al*. Closing two doors of viral entry: intramolecular combination of a coreceptor- and fusion inhibitor of HIV-1. Virol J. 2008;5:56.
6. Ji C, Kopetzki E, Jekle A, Stubenrauch KG, Liu X, Zhang J, *et al*. CD4-anchoring HIV-1 fusion inhibitor with enhanced potency and *in vivo* stability. J Biol Chem. 2009;284(8):5175–85.
7. Jekle A, Chow E, Kopetzki E, Ji C, Yan MJ, Nguyen R, *et al*. CD4-BFFI: a novel, bifunctional HIV-1 entry inhibitor with high and broad antiviral potency. Antivir Res. 2009;83(3):257–66.
8. Boon L, Holland B, Gordon W, Liu P, Shiau F, Shanahan W, *et al*. Development of anti-CD4 MAb hu5A8 for treatment of HIV-1 infection: preclinical assessment in non-human primates. Toxicology. 2002;172(3):191–203.
9. Kuritzkes DR, Jacobson J, Powderly WG, Godofsky E, DeJesus E, Haas F, *et al*. Antiretroviral activity of the anti-CD4 monoclonal antibody TNX-355 in patients infected with HIV type 1. J Infect Dis. 2004;189(2):286–91.

10. Burkly LC, Olson D, Shapiro R, Winkler G, Rosa JJ, Thomas DW, *et al*. Inhibition of HIV infection by a novel CD4 domain 2-specific monoclonal antibody. Dissecting the basis for its inhibitory effect on HIV-induced cell fusion. J Immunol. 1992;149(5):1779–87.
11. Mager DE, Jusko WJ. General pharmacokinetic model for drugs exhibiting target-mediated drug disposition. J Pharmacokinet Pharmacodyn. 2001;28(6):507–32.
12. Ng CM, Stefanich E, Anand BS, Fielder PJ, Vaickus L. Pharmacokinetics/pharmacodynamics of nondepleting anti-CD4 monoclonal antibody (TRX1) in healthy human volunteers. Pharm Res. 2006;23(1):95–103.
13. Mager DE. Target-mediated drug disposition and dynamics. Biochem Pharmacol. 2006;72(1):1–10.
14. Oitate M, Masubuchi N, Ito T, Yabe Y, Karibe T, Aoki T, *et al*. Prediction of human pharmacokinetics of therapeutic monoclonal antibodies from simple allometry of monkey data. Drug Metab Pharmacokinet. 2011;26(4):423–30.
15. Lobo ED, Hansen RJ, Balthasar JP. Antibody pharmacokinetics and pharmacodynamics. J Pharm Sci. 2004;93(11):2645–68.
16. Hinton PR, Xiong JM, Johlfs MG, Tang MT, Keller S, Tsurushita N. An engineered human IgG1 antibody with longer serum half-life. J Immunol. 2006;176(1):346–56.
17. Zheng Y, Scheerens H, Davis Jr JC, Deng R, Fischer SK, Woods C, *et al*. Translational pharmacokinetics and pharmacodynamics of an FcRn-variant anti-CD4 monoclonal antibody from preclinical model to phase I study. Clin Pharmacol Ther. 2011;89(2):283–90.
18. Pelchen-Matthews A, Armes JE, Griffiths G, Marsh M. Differential endocytosis of CD4 in lymphocytic and nonlymphocytic cells. J Exp Med. 1991;173(3):575–87.
19. Dong JQ, Salinger DH, Endres CJ, Gibbs JP, Hsu CP, Stouch BJ, *et al*. Quantitative prediction of human pharmacokinetics for monoclonal antibodies: retrospective analysis of monkey as a single species for first-in-human prediction. Clin Pharmacokinet. 2011;50(2):131–42.
20. Deng R, Iyer S, Theil FP, Mortensen DL, Fielder PJ, Prabhu S. Projecting human pharmacokinetics of therapeutic antibodies from nonclinical data: what have we learned? mAbs. 2011;3(1):61–6.
21. Ling J, Zhou H, Jiao Q, Davis HM. Interspecies scaling of therapeutic monoclonal antibodies: initial look. J Clin Pharmacol. 2009;49(12):1382–402.
22. Lin K, Tibbitts J. Pharmacokinetic considerations for antibody drug conjugates. Pharm Res. 2012;29(9):2354–66.
23. Luu KT, Bergqvist S, Chen E, Hu-Lowe D, Kraynov E. A model-based approach to predicting the human pharmacokinetics of a monoclonal antibody exhibiting target-mediated drug disposition. J Pharmacol Exp Ther. 2012;341(3):702–8.
24. Aiken C, Konner J, Landau NR, Lenburg ME, Trono D. Nef induces CD4 endocytosis: requirement for a critical dileucine motif in the membrane-proximal CD4 cytoplasmic domain. Cell. 1994;76(5):853–64.
25. Rhee SS, Marsh JW. Human immunodeficiency virus type 1 Nef-induced down-modulation of CD4 is due to rapid internalization and degradation of surface CD4. J Virol. 1994;68(8):5156–63.
26. Schwartz O, Dautry-Varsat A, Goud B, Marechal V, Subtil A, Heard JM, *et al*. Human immunodeficiency virus type 1 Nef induces accumulation of CD4 in early endosomes. J Virol. 1995;69(1):528–33.
27. Schwartz O, Marechal V, Le Gall S, Lemonnier F, Heard JM. Endocytosis of major histocompatibility complex class I molecules is induced by the HIV-1 Nef protein. Nat Med. 1996;2(3):338–42.
28. Reimann KA, Lin W, Bixler S, Browning B, Ehrenfels BN, Lucci J, *et al*. A humanized form of a CD4-specific monoclonal antibody exhibits decreased antigenicity and prolonged plasma half-life in rhesus monkeys while retaining its unique biological and antiviral properties. AIDS Res Hum Retrovir. 1997;13(11):933–43.
29. Schellekens PT, Tersmette M, Roos MT, Keet RP, de Wolf F, Coutinho RA, *et al*. Biphasic rate of CD4+ cell count decline during progression to AIDS correlates with HIV-1 phenotype. AIDS. 1992;6(7):665–9.